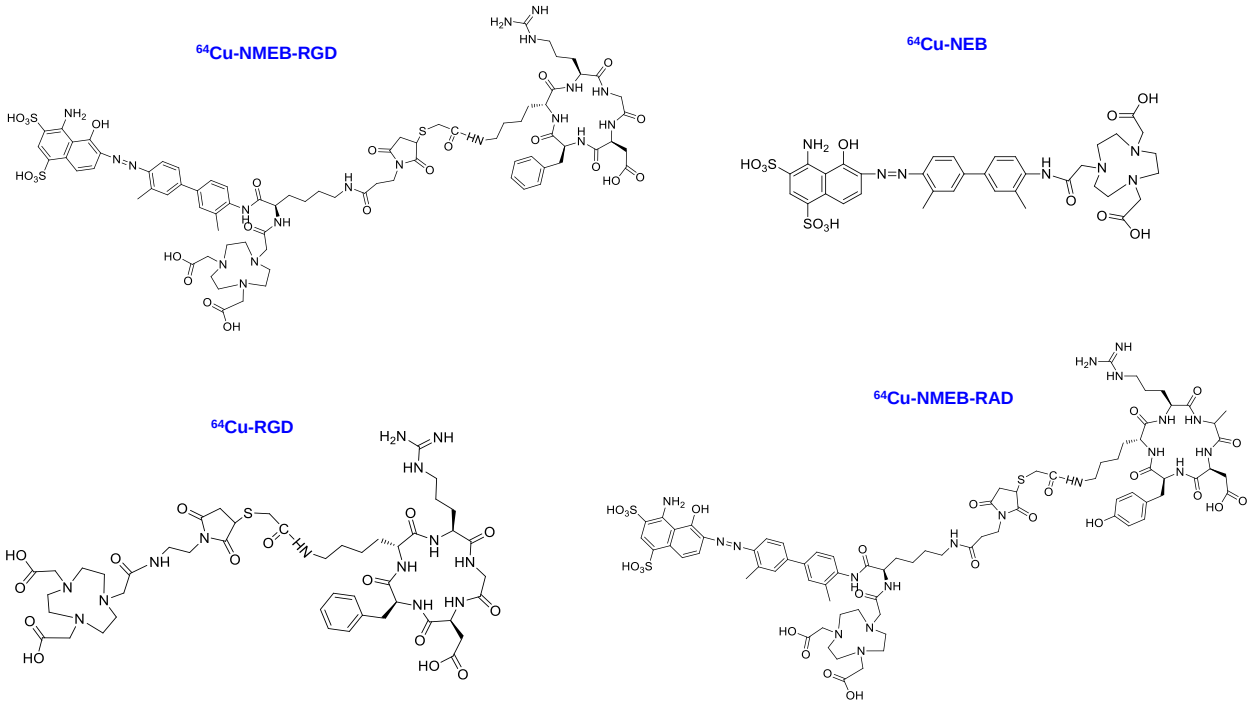

Supplemental Figure 1. Chemical structure of ^{64}Cu-NMEB-RGD (contains EB entity for albumin binding and RGD peptide as integrin $\alpha_v\beta_3$-positive), ^{64}Cu-NEB (contains only EB part with no specificity to integrin $\alpha_v\beta_3$), ^{64}Cu-RGD (integrin $\alpha_v\beta_3$-positive but does not have albumin binding), and ^{64}Cu-NMEB-RAD (contains albumin motif, EB, and integrin $\alpha_v\beta_3$-negative).

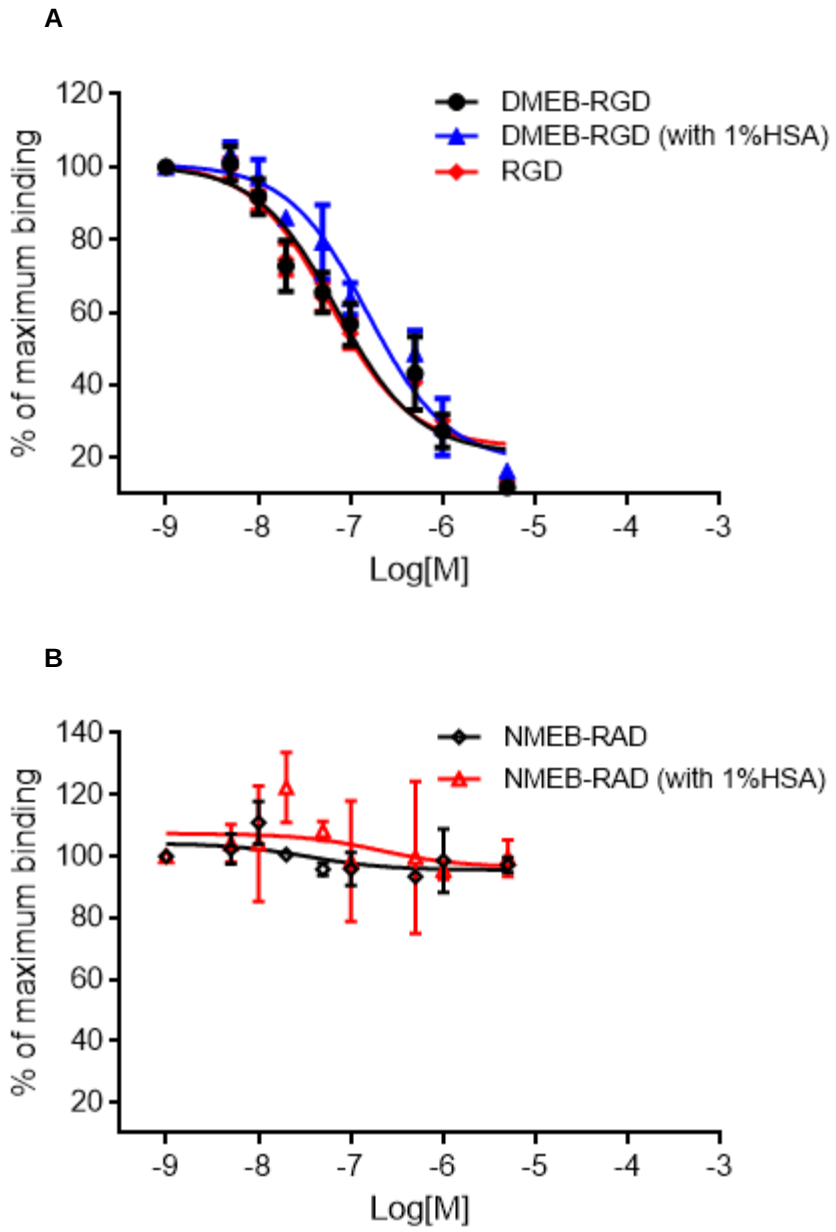

Supplemental Figure 2. Cell binding assay in U87MG cells using ^{64}Cu-RGD as a competitor and 4-h incubation time of DMEB-RGD (A) and (B) NMEB-RAD with or without 1% HSA.

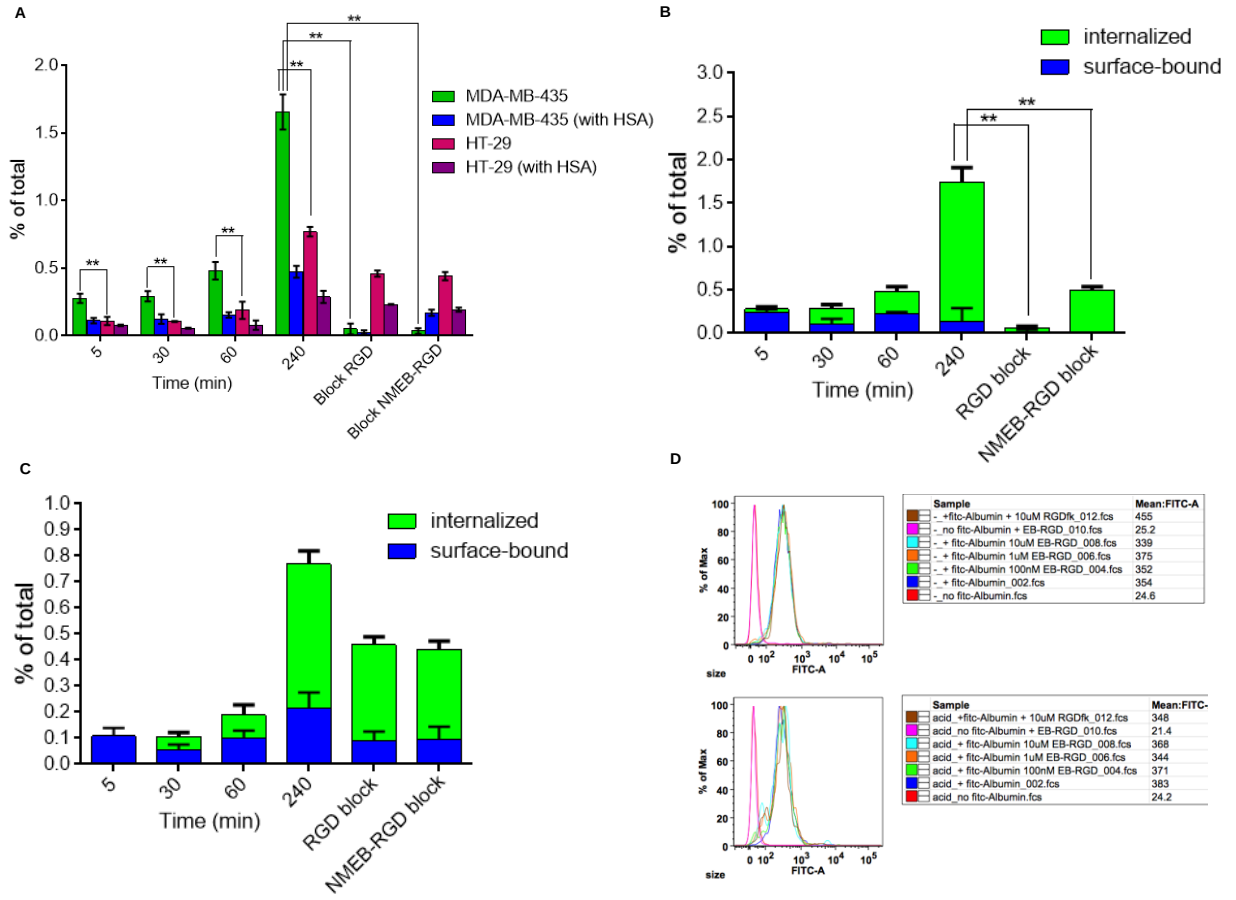

Supplemental Figure 3. (A) Cell uptake of ^{64}Cu-NMEB-RGD in MDA-MB-435 and HT-29 cells without HSA and with 1% HSA. Blocking studies were evaluated at 4 h. (B) Cell internalization of ^{64}Cu-NMEB-RGD in MDA-MB-435 cell line (C) and HT-29 cell line. Green bars represent the internalized radiotracer, and blue bars represent surface-bound ^{64}Cu-NMEB-RGD. Blocking studies were evaluated at 4 h. $^{**}P < 0.01$. (D) Lack of internalization of FITC-albumin in the presence of increasing concentrations of NMEB-RGD with (upper) and without (lower) acid wash.

A

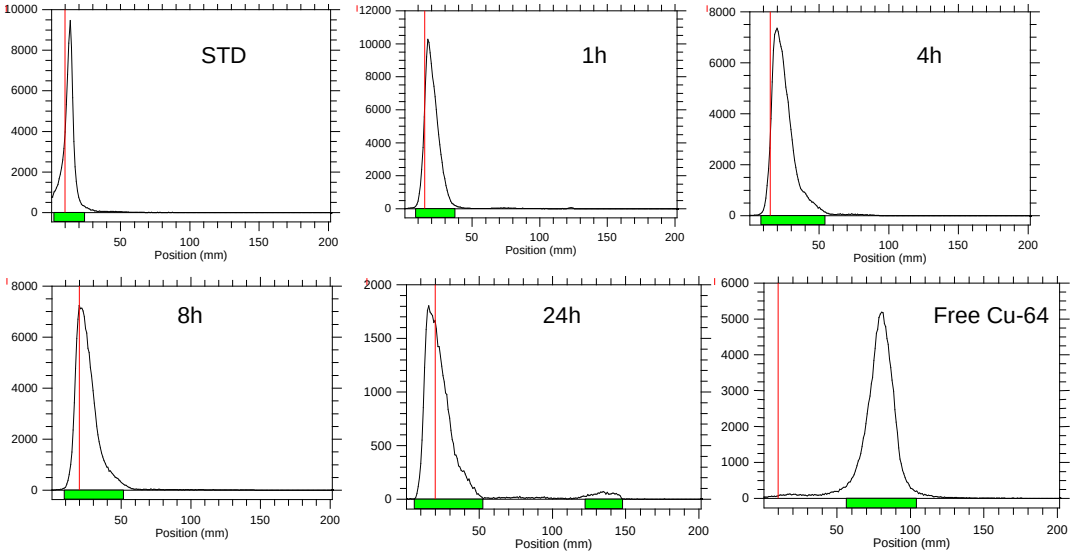

B

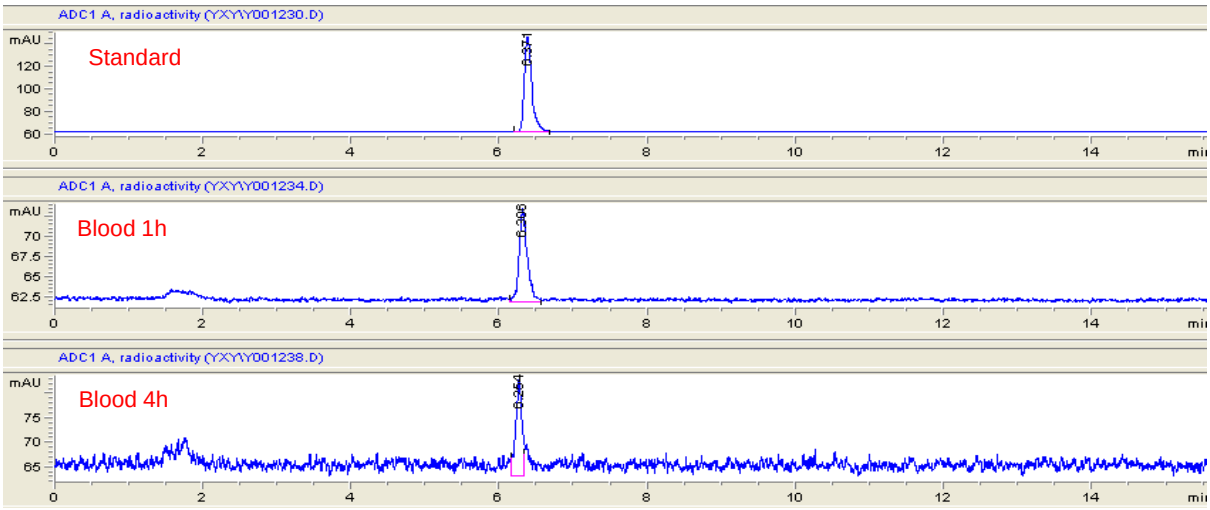

Supplemental Figure 4. (A) Stability of ^{64}Cu-NMEB-RGD in mouse serum over time using radio-TLC and in vivo in mouse blood (B) analyzed by radio-HPLC.

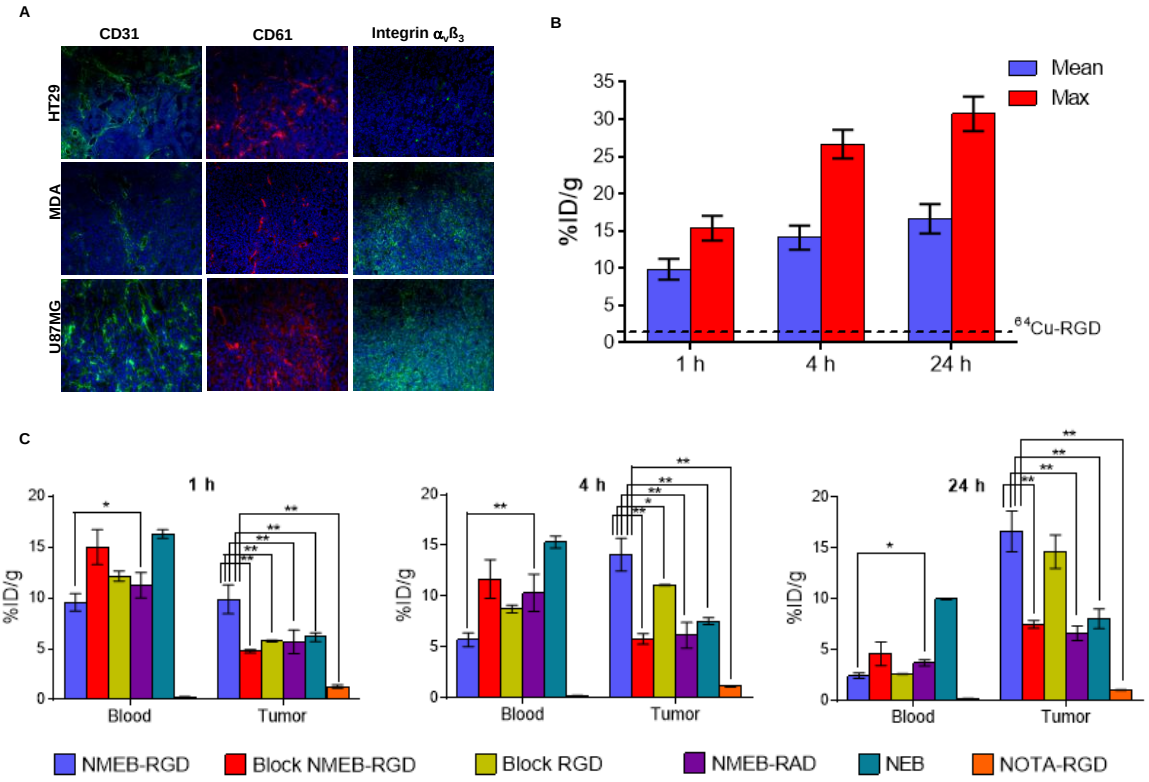

Supplemental Figure 5. (A) Immunofluorescence staining of CD31, CD61 (murine integrin β3) and human integrin $\alpha_v\beta_3$in frozen section slides of U87MG, MDA-MB-435, and HT29 xenografts. Magnification is ×200. (B) Quantified uptake of ^{64}Cu-NMEB-RGD in U87MG tumors. PET quantification was done as both mean tumor uptake and maximum tumor uptake to compensate for necrotic areas that might affect the calculated mean. (C) Quantified results for PET presented in Fig. 3 at different time points. *$P < 0.05$, **$P < 0.01$.

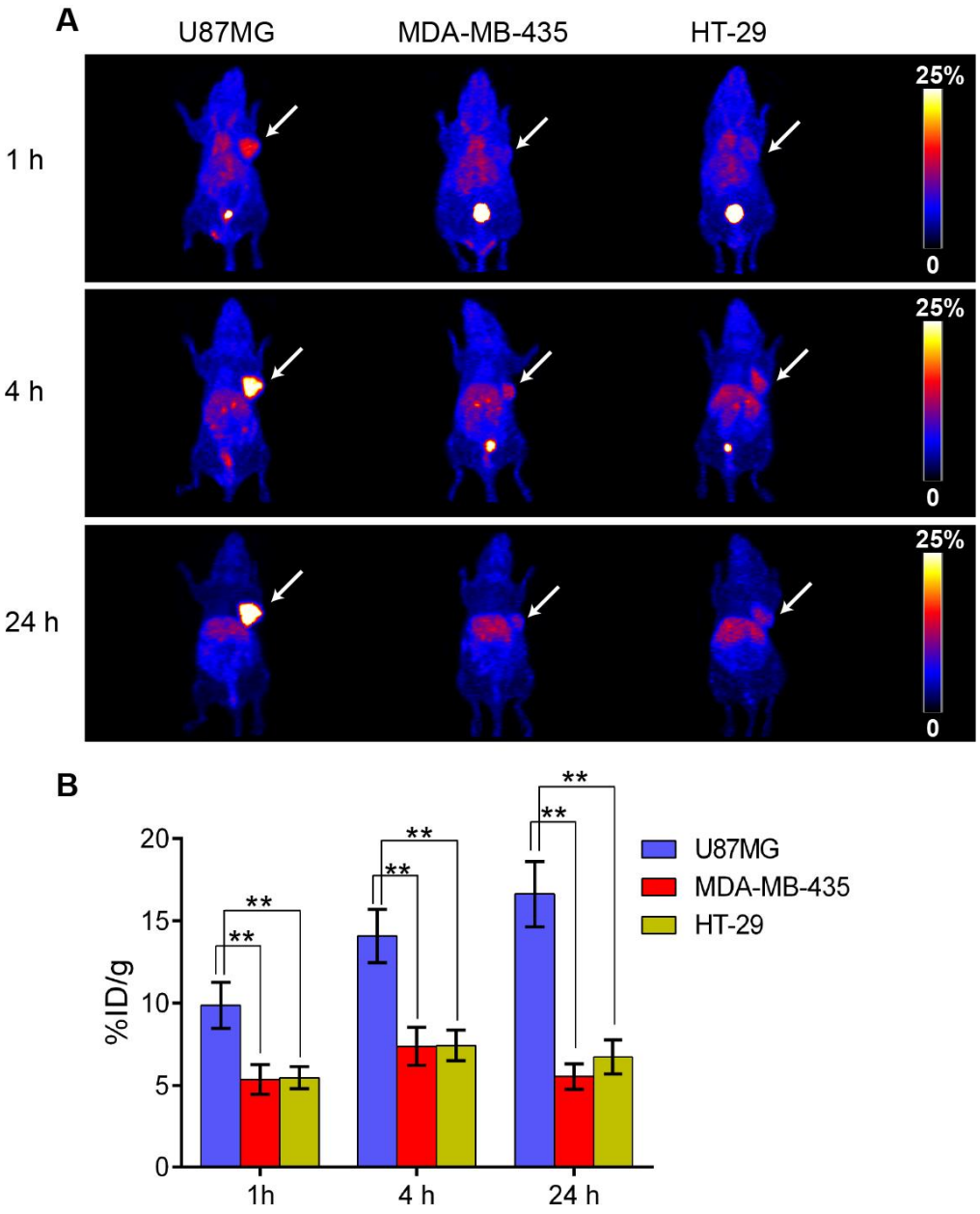

Supplemental Figure 6. Comparison of ^{64}Cu-NMEB-RGD uptake in different tumors. (A) Projection PET images of mice bearing tumors with different integrin $\alpha_v\beta_3$ levels injected with 3.7 MBq (100 µCi) of ^{64}Cu-NMEB-RGD at 1, 4, and 24,h p.i. White arrows indicate the tumor location. (B) PET quantification of the images. $^{**}P < 0.01$.

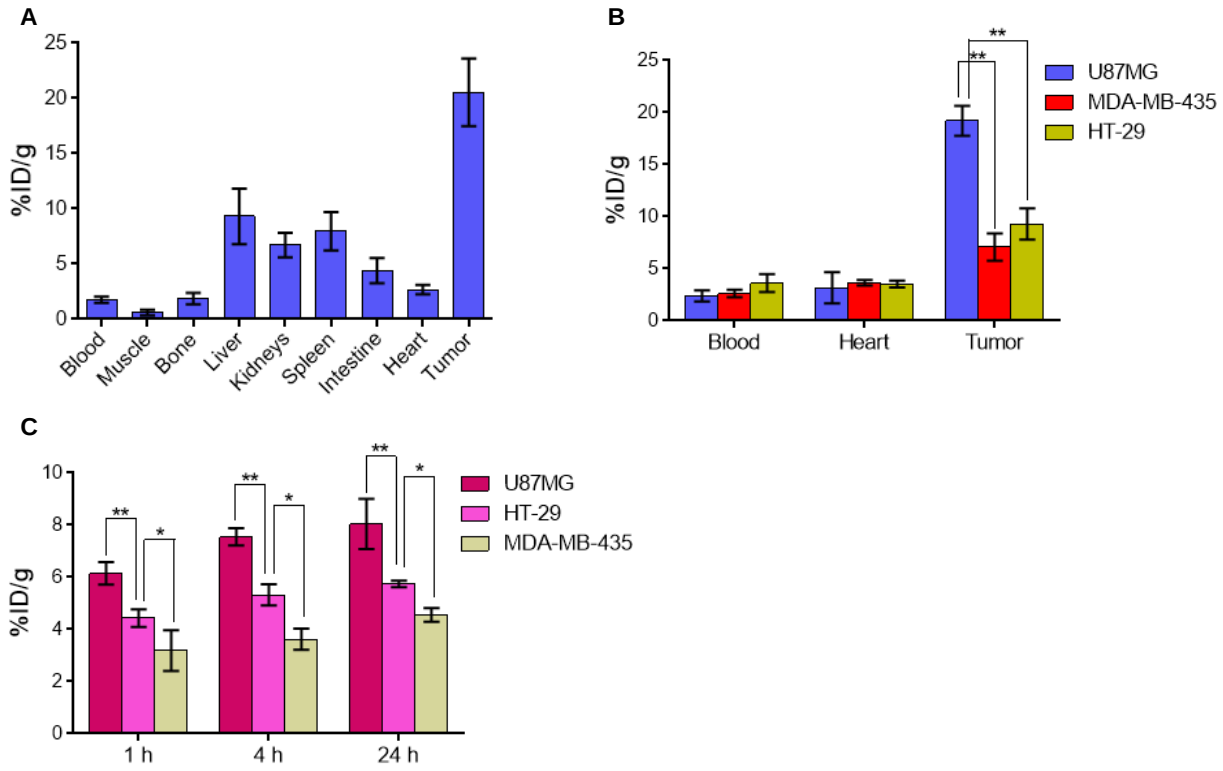

Supplemental Figure 7. (A) Biodistribution of ^{64}Cu-NMEB-RGD in U87MG xenografts at 4 h after injection. (B) Biodistribution comparison of blood, heart, and tumor uptake of ^{64}Cu-NMEB-RGD. (C) ^{64}Cu-NEB in different integrin $\alpha_v\beta_3$-expressing tumors. *P < 0.05, **P < 0.01.

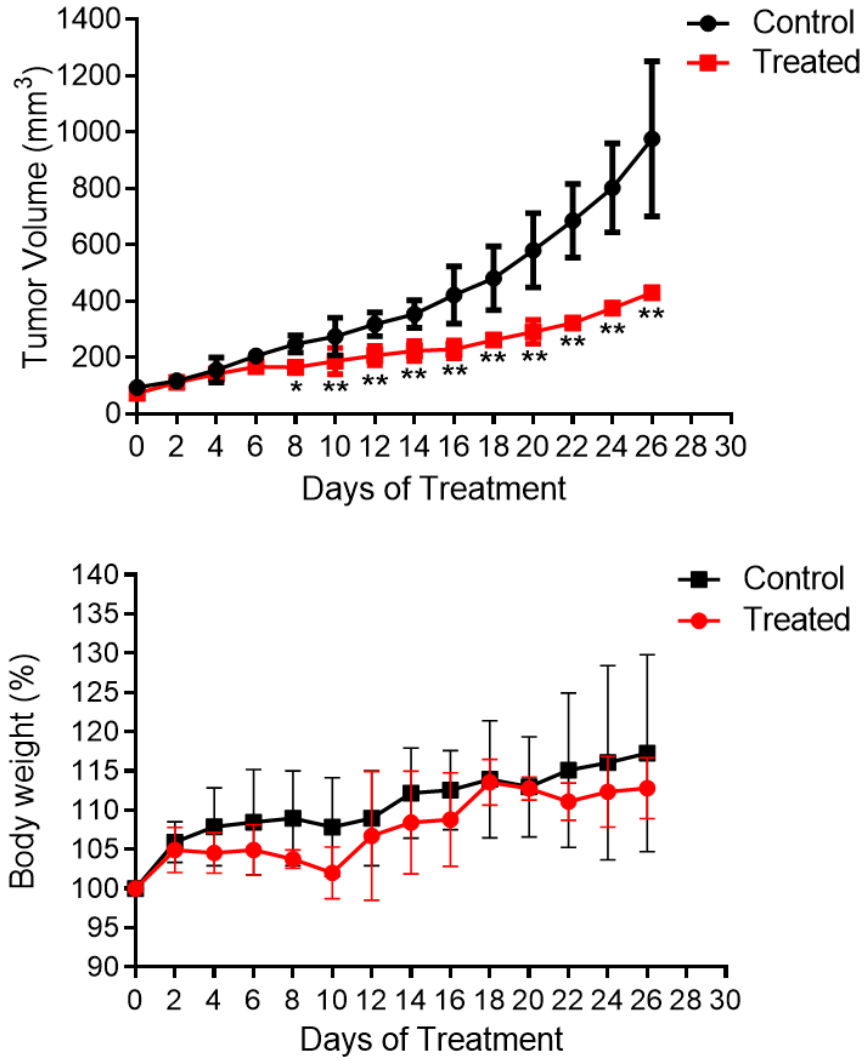

Supplemental Figure 8. **Cancer radiotherapy using ^{90}Y-DMEB-RGD in HT-29 xenografts.** (A) Tumor volume growth and (B) body weight changes of mice injected with either; saline (control) and 200 µCi of ^{90}Y-DMEB-RGD (treated). Treatment initiated at day 0.